Econ. Environ. Geol.
Vol. 29, No. 3, p. 281-291, 1996.

Geochemistry and Petrogenesis of the Badwater Greenstones from Crystal Falls Terrane in Northeastern Wisconsin, U.S.A.

Soo-Meen Wee*

ABSTRACT : Samples of Badwater greenstones from the Crystal Falls terrane in northeastern Wisconsin have been analyzed for major, trace and rare earth elements. Geochemical characteristics of the rocks provide clues to the petrologic character and paleotectonic environment of basaltic magma generation. They have chemical composition typical of continental tholeiites. The low Mg values and abundances of Ni and Cr indicate that the lavas were extensively fractionated prior to extrusion. The variations of incompatible elements suggest that the rocks were affected by interaction with crustal rocks. The samples least affected by contamination have trace element compositions similar to those of T-type mid-ocean ridge basalts. The parent was modified by crustal contamination process and this process shifted the rock compositions to that of continental tholeiites as the rock evolved. Interpretations of the chemical characteristics of the rocks, based on modern analogs, favor their emplacement in an extensional tectonic regime.

INTRODUCTION

Two major early Proterozoic tectonic provinces in the southern Lake Superior region (Figure 1), the northern passive margin terrane, and the southern magmatic arc terrane, have given rise to controversial interpretations of their tectonic evolution such as plate margin model (Van Schmus, 1976) and arc-continent collision model (Cambray, 1978; Greenberg and Brown, 1983; Larue and Ueng, 1985). The arc-continent collision model proposes that the nothern passive margin terrane was subducted below and accreted to the southern magmatic arc terrane during the Penokean Orogeny (1.85~1.9 Ga). However, Van Schmus (1976) proposed that the northern terrane represents a back-arc or foreland basin assemblage and that the southern magmatic arc terrane is a remnant of a Proterozoic Andean-type continental margin.

It has been recognized that volcanic rocks erupted within specific tectonic settings possess distinctive trace element and, in some cases, major element signatures. The early Proterozoic dikes, Hemlock volcanics, which are part of passive margin terrane, and the Badwater greenstones of Crystal Falls terrane, which lying between the passive margin terrane and magmatic arc terrane, represent a volcanic and intrusive stage in the formation of this geologically complex area. The geochemical study of the dikes and the Hemlock volcanics have been carried out by many workers (Fox, 1983; Ueng *et al.*, 1988; Wee, 1991, 1993). However, previous studies of the Badwater greenstones in Crystal Falls terrane are few and could not be used to evaluate petrogenesis and tectonic environment of magma generation. The significance of the petrogenetic origin of the Badwater greenstones is as profound as that of the dikes and the Hemlock volcanics in order to understand paleotectonic environment of the southern part of the Lake Superior region.

Thus, this investigation is focused on the geochemistry of the early Proterozoic Badwater greenstones of Crystal Falls terrane in the northeastern Wisconsin. The combination of these geochemical results with the available geological information provides additional clues for unravelling the development of the past local tectonic framework, and this paper served as a part of the study for the reconstruction of the paleotectonic environment of southern Lake Superior region in North America craton.

* Department of Earth Science Education, Korea National University of Education, Chungbuk 363-791, Korea

REGIONAL GEOLOGY

Geological Setting

The Precambrian geology of the northern Michigan and northeastern Wisconsin is very complex and is related to several tectonic events. The area has been involved in two major orogenic

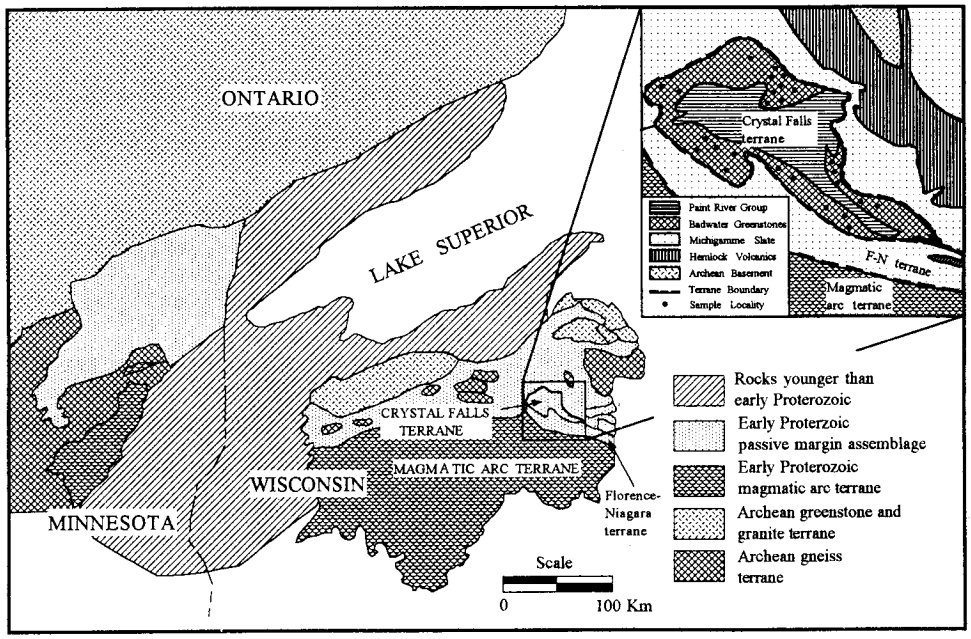

Fig. 1. General geology and the early Proterozoic tectonostratigraphic terranes in the southern Lake Superior region(After Ueng *et al.*, 1988).

episodes, the Algoman Orogeny (2.7 Ga) and the Penokean Orogeny, which occured about 1.85~1.9 Ga ago and included deformation, metamorphism, and extrusive and intrusive igneous activities (Cannon, 1973; Van Schmus, 1976). The area was divided into four tectonostratigraphic terranes by Larue (1983), such as the passive margin terrane, the Crystal Falls terrane, the Florence-Niagara terrane, and the magmatic arc terrane.

The passive margin terrane is composed of three transgressive metasedimentary sequences deposited unconformably on Archean sialic crust. The metasedimentary sequence, from the oldest to youngest, are the Chocolay, the Menominee and the Baraga group. The Crystal Falls terrane is composed of the Paint River group and underlying Badwater greenstones, a thick units of pillow basalts and greenstones. The contact of the Paint River group with the underlying Badwater greenstones has been inferred to be a fault along the northern border of the Crystal Falls terrane (Larue, 1983), or uncomformity (James *et al.*, 1968). The Florence-Niagara terrane consists of eight major fault-bounded packets that strike E-W to NW-SE. The fault-bounded packets containing highly deformed rocks that are, for the most part, correlative with the passive margin terrane. The Florence-Niagara terrane has been interpreted as a fragment of the passive margin terrane which was accreted to the forearc area of the magmatic terrane during the Penokean arc-continent collision (Larue, 1983; Larue and Ueng, 1985; Ueng *et al.*, 1988). The magmatic arc terrane consists of several cores of granitoid to gneissic rocks mantled by highly deformed metavolcanic, metapellitic, and meta-gabbroic rocks. The early Proterozoic dike swarms are exposed mostly in the passive margin terrane with various orientations.

Description of the Badwater greenstones

The Badwater greenstone is the youngest unit in the Baraga group. The greenstone was formed, for the most part, by the metamorphism of pillow lavas and tuffaceous and agglomeratic phases, which indicate deposition in a subaqueous environment. The greenstones are generally massive chloritized basaltic flows but locally ellipsoidal or slightly foliated. The Badwater greenstone consists of plagioclase, amphibole (actinolite and hornblende), chlorite, epidote and clinozoisite as the major constituents; biotite, quartz, and carbonate are minor constituents. Most plagioclase occures as micro-phenocrysts, but medium sized grains are also found in the samples from the interior of the flows. Most plagioclase grains are altered to sericite as well as clinozoisite and epidote, and are often partially

Table 1. Major, trace and rare earth element analyses of Badwater greenstones.

	SiO_2	Al_2O_3	FeO	MnO	MgO	CaO	Na_2O	K_2O	TiO_2	P_2O_5	Total	Ni	Cu	Cr	Zn	Rb
CF-1	47.36	16.85	11.11	0.16	8.13	8.24	2.92	0.34	1.36	0.12	96.59	124.5	35.4	344.9	90.1	3.2
CF-2	52.23	13.62	12.47	0.17	3.62	8.92	1.94	0.82	1.76	0.23	95.78	24.6	49.2	22.3	108.3	15.3
CF-3	50.30	13.90	13.42	0.20	5.45	9.55	2.11	0.07	1.31	0.12	96.43	44.2	100.9	51.5	107.1	1.0
CF-4	50.88	13.24	12.53	0.19	5.07	10.57	1.92	0.09	1.25	0.12	95,86	48.1	132.9	51.5	96.6	1.3
CF-5	50.00	14.51	11.70	0.18	5.43	10.68	2.64	0.04	1.23	0.11	96.52	52.0	36.3	77.6	91.4	1.2
CF-6	51.29	14.52	12.85	0.20	5.91	7.16	2.10	0.92	1.40	0.12	96.47	47.0	80.0	117.7	109.5	12.5
FLE-2	47.48	15.88	10.60	0.16	4.76	6.95	0.29	0.08	1.40	0.13	97.73	93.7	187.7	258.1	63.9	1.1
FLE-3	45.98	15.05	12.69	0.20	7.86	11.29	1.78	0.26	1.66	0.16	96.93	151.0	136.5	30.8	99.3	2.3
FLE-4	51.29	14.18	12.21	0.18	6.81	7.03	3.38	0.54	1.36	0.18	97.16	50.2	57.2	64.1	91.5	9.5
FLE-5	52.50	17.26	8.76	0.13	4.30	4.56	5.16	1.63	1.53	0.17	96.00	56.1	45.6	135.6	114.2	34.8
FLE-6	51.70	14.98	13.01	0.17	5.23	4.26	3.42	0.74	2.54	0.30	96.35	23.8	0.1	128.0	127.0	12.5
FLE7A	49.44	14.94	9.90	0.18	7.62	12.22	1.92	0.21	1.12	0.14	97.69	91.2	60.8	368.1	73.0	1.8
FLE7B	52.04	14.32	7.43	0.14	7.31	10.26	3.77	0.41	1.19	0.17	97.04	99.4	57.8	315.7	73.3	2.3
FLE-8	50.95	14.85	8.89	0.15	7.37	10.98	2.47	0.42	0.97	0.10	97.15	73.9	86.1	320.4	75.8	8.3
FLE-9	49.47	14.52	10.13	0.17	7.74	12.76	1.32	0.48	1.07	0.10	97.76	86.9	65.3	109.5	71.3	8.1
FLW-1	47.14	15.59	12.40	0.18	6.10	12.12	1.08	0.34	1.56	0.14	96.65	134.9	163.9	232.5	111.9	7.5
FLW-2	48.14	15.64	11.83	0.17	5.41	11.08	1.77	0.37	1.54	0.15	97.10	118.1	119.8	290.1	86.8	6.7
FLW-3	47.14	15.42	12.27	0.18	5.76	10.20	2.10	0.66	2.25	0.27	96.25	84.0	167.6	197.3	92.3	7.0
IM-1	50.81	13.76	14.25	0.21	4.88	6.06	1.92	1.86	2.01	0.27	96.03	49.3	68.0	148.8	121.0	37.8
IM-2	43.79	17.27	14.36	0.20	6.05	8.76	1.79	0.20	1.87	0.17	94.46	43.1	201.3	123.4	94.6	2.2
IM-3A	48.02	15.99	9.21	0.14	4.43	8.49	3.46	0.34	1.28	0.12	96.48	58.2	159.8	163.9	62.2	3.2
IM-3B	44.85	17.38	12.19	0.19	5.74	11.54	2.52	0.12	1.74	0.16	96.43	67.5	111.3	244.1	93.6	2.0
IM-3C	47.53	12.54	15.35	0.25	5.25	10.17	2.32	0.31	2.37	0.25	96.34	32.9	248.9	172.0	127.6	5.6
IM-4	47.21	15.80	10.69	0.17	9.51	8.39	2.18	0.69	1.13	0.12	95.89	280.8	124.6	179.2	75.4	12.2
IM-5	48.54	15.55	12.14	0.18	6.54	8.82	2.21	0.61	1.70	0.16	96.45	110.8	176.3	228.6	94.5	7.2
IM-6A	49.61	15.99	12.23	0.17	8.01	6.82	1.60	0.36	1.37	0.10	96.26	154.2	137.6	272.0	82.3	5.0
IM-7	41.61	14.58	12.39	0.20	5.45	6.58	3.90	1.20	1.47	0.16	97.54	36.4	48.4	133.3	98.9	12.6
CP-1*	69.26	15.57	3.47	0.04	1.80	1.89	2.93	3.15	0.44	0.13	98.68	7.9	14.6	5.3	71.7	94.2
WL-3*	72.08	11.51	4.00	0.06	0.49	1.06	2.76	4.30	0.56	0.09	96.91	0.0	92.4	11.4	70.7	86.4
WF-6*	74.09	14.09	1.36	0.02	0.35	1.22	4.53	3.49	0.15	0.05	99.35	0.0	1.9	0.1	38.1	65.5

Note : major element analyses are in wt. percent, trace and REE analyses are in parts per million, FeO represents total iron, *; archean granite

replaced by carbonate. The groundmass usually consists of chlorite and very fine grained aggregates of epidote, clinozoisite, and carbonate.

SAMPLING AND ANALYTICAL METHODS

In this study, sampling was focused on the Badwater greenstones in Crystal Falls terrane. Twenty seven samples from Badwater greenstone and three supracrustal rocks were collected. Whole rock samples from the Badwater greenstones and the basement rocks were analyzed for major and selected trace elements, including rare earth elements (REE). Results of the chemical analyses are listed in Table 1. Standard X-ray fluorescense (XRF) and Instrumental Neutron Activation Analyses (INAA) procedures developed at Michigan State University were used to determine whole rock compositions of the major, trace elements, and REE. Major and trace elements such as Rb, Sr, Nb, Y, Cr, Ni, Cu, Zn, and Zr were analyzed by XRF. REE and Th, Sc, and Hf were analyzed by INAA.

Accuracy for major elements is within 2% except for P, which is 5.4%. Trace elements by XRF are accurate to within 5% except for Y and Zn, which are less than 10%. Accuracy for elements by INAA is less than 10%, but where concentrations are less than 10 ppm (Tb, Lu, and Th), accuracy approaches 15%.

ANALYTICAL RESULTS

Major element

Analyzed rocks were plotted on a $Na_2O + K_2O$ versus $100 \times K_2O/(K_2O+Na_2O)$ diagram (Hughes, 1973) which is useful to evaluate the effects of secondary alteration (Figure 2). Rocks whose compositions lie outside the envelope ("igneous spectrum") are probably due to element mobility

Table 1. Continued.

	Sr	Y	Sc	Zr	Nb	Ba	La	Ce	Sm	Eu	Tb	Yb	Lu	Hf	Th
CF-1	255.2	18.6	37.0	110.8	10.8	76.4	11.32	26.83	3.55	1.12	0.66	1.85	0.33	2.65	3.85
CF-2	455.4	28.0	36.1	185.9	9.8	243.6	28.84	63.39	6.02	1.88	0.83	2.62	0.43	4.56	7.12
CF-3	442.4	20.4	44.3	117.8	6.8	38.6	15.11	30.75	3.50	1.23	0.66	2.32	0.42	2.56	3.50
CF-4	425.5	19.8	44.2	113.6	5.7	30.4	11.74	27.80	3.52	1.19	0.61	2.04	0.37	2.40	3.61
CF-5	304.3	19.6	45.4	98.2	7.2	38.0	11.56	24.50	3.32	1.23	0.47	1.72	0.36	2.35	2.52
CF-6	204.9	23.5	39.7	110.0	10.3	896.5	15.90	28.73	3.99	2.32	0.84	2.71	0.42	8.36	9.70
FLE-2	524.0	18.9	35.2	108.9	4.0	35.3	8.76	22.69	3.39	1.17	0.52	1.80	0.37	2.66	2.66
FLE-3	207.7	20.3	39.1	102.8	10.1	57.0	10.35	27.49	3.76	1.23	0.58	2.12	0.38	2.93	1.83
FLE-4	115.3	20.6	34.5	134.4	12.8	113.1	13.95	29.91	3.24	1.22	0.60	1.80	0.36	3.46	3.82
FLE-5	150.0	29.6	33.0	130.7	10.1	506.0	31.73	71.07	4.05	2.12	0.67	2.33	0.38	5.65	3.40
FLE-6	192.2	34.2	42.6	210.9	25.1	523.1	40.88	102.45	7.70	2.70	1.02	2.64	0.23	3.74	11.85
FLE7A	341.5	18.1	35.5	92.4	8.6	88.1	10.12	27.59	3.23	2.08	0.77	2.38	0.41	5.54	4.87
FLE7B	150.7	18.6	42.6	88.4	11.8	190.2	13.99	31.39	3.29	0.99	0.58	2.11	0.36	2.17	3.63
FLE-8	230.7	17.4	36.3	80.4	7.5	121.1	10.46	26.48	3.33	1.92	0,73	2.33	0.40	4.99	5.28
FLE-9	196.8	18.5	35.8	78.2	10.3	112.1	22.31	52.38	6.59	2.12	0.74	2.46	0.40	7.04	6.06
FLW-1	238.1	20.9	33.6	102.2	8.8	128.0	10.73	26.97	3.36	2.26	0.73	2.41	0.40	5.97	4.02
FLW-2	188.6	21.6	31.2	96.1	9.9	279.6	10.38	27.23	3.35	2.23	0.78	2.49	0.37	6.40	5.66
FLW-3	279.7	27.5	33.7	158.1	16.3	544.0	17.93	30.49	5.45	2.94	0.83	2.65	0.39	9.40	7.69
IM-1	204.6	33.7	33.4	187.4	18.3	1340.5	27.58	33.72	7.21	2.58	0.88	2.64	0.39	5.48	7.38
IM-2	370.9	24.6	47.8	132.9	11.0	50.2	17.00	43.15	4.65	1.80	0.86	1.94	0.40	3.47	4.26
IM-3A	263.4	18.1	27.0	89.6	13.2	63.9	10.89	19.98	2.94	1.63	0.40	1.81	0.26	2.21	1.94
IM-3B	244.7	20.3	50.7	110.3	9.8	93.9	16.04	26.77	6.24	2.33	0.69	2.35	0.35	2.95	2.59
IM-3C	216.9	30.0	31.1	155.6	19.0	160.1	14.31	33.35	3.15	2.87	0.99	2.91	0.45	3.66	3.20
IM-4	183.2	18.8	46.4	81.8	12.7	253.2	18.27	20.50	3.45	1.60	0.42	1.83	0.28	5.22	2.00
IM-5	185.4	22.9	34.4	109.9	15.8	190.5	16.62	25.40	2.96	1.58	0.65	2.34	0.35	5.06	3.07
IM-6A	161.3	19.8	37.8	81.8	12.5	121.3	11.36	24.84	5.15	1.99	0.66	2.30	0.36	4.59	2.78
IM-7	188.4	25.2	30.3	137.5	25.8	537.9	9.46	30.24	3.75	2.05	0.81	2.48	0.38	7.47	6.00
CP-1*	228.7	21.2	27.6	123.4	5.0	581.7	50.11	51.41	5.09	0.34	0.36	1.76	0.14	12.05	6.52
WL-3*	58.7	44.0	9.7	303.2	23.4	994.0	45.12	73.28	9.77	1.60	0.40	1.40	0.24	3.29	0.10
WF-6*	502.6	18.3	16.9	176.1	0.0	913.3	29.30	26.61	4.89	0.62	0.10	1.80	0.11	1.94	0.10

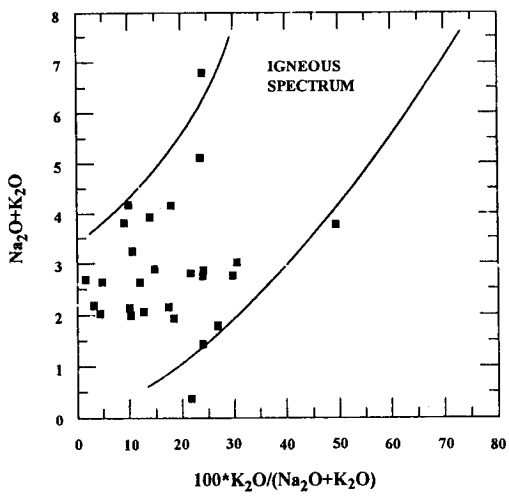

Fig. 2. Badwater greenstones on a alkai vs $100\times K_2O/(K_2O+Na_2O)$ diagram. Igneous spectrum (area between solid lines) represents the range of variation of vairous modern volcanic rocks.

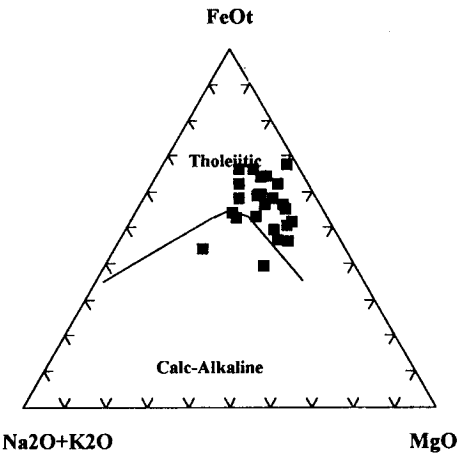

Fig. 3. AFM diagram for the Badwater greenstones.

during secondary and metamorphic alteration (Honkamo, 1987). Although the diagram shows a few conspicuously deviating samples, the plots of

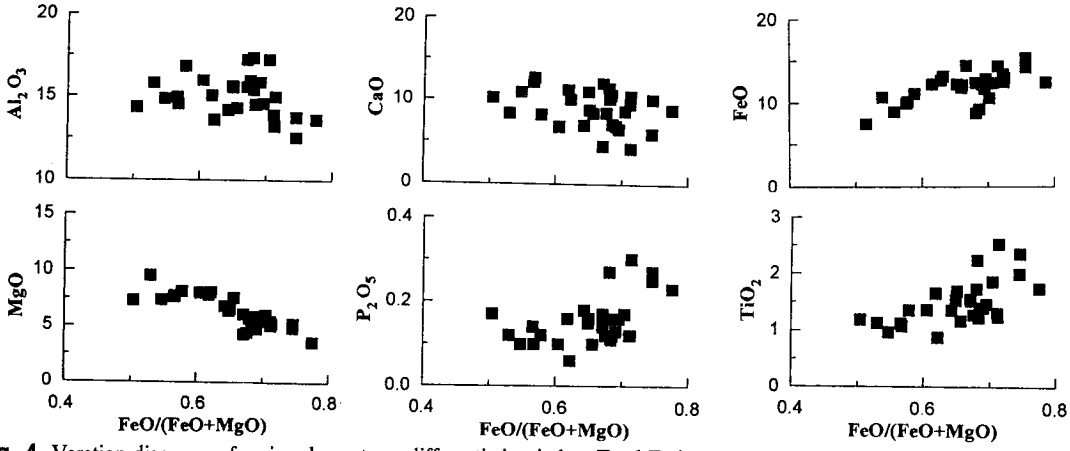

Fig. 4. Varation diagrams of major elements vs differentiation index. Total Fe is reported as FeO.

the rocks from the study area fall well within the field of modern volcanic suites on this diagram, indicating that metamorphic alteration has only been minimal.

The analyzed rocks have mostly basaltic compositions with a relatively wide range of SiO_2 (43. 7~52.5%), and majority of the rocks fall within the tholeiitic field in an AFM diagram (Figure 3). Major and trace element composition of the rocks are similar to that of continental tholeiites. The Mg numbers (MgO/(MgO + FeO); FeO represents total iron) of the rocks vary between 64 to 40 show a relatively narrow range (mostly in 40 to 50). These relatively low Mg numbers indicate significant fractionation of the magma, and such evolved compositions are typical of Precambrian basaltic rocks from other localities (Condie *et al.*, 1987).

Differentiation trends for the Badwater greenstones are shown in Figure 4. The abundances of TiO_2, P_2O_5, and FeO increase with increasing with differentiation index, while MgO, CaO, Al_2O_3 decrease. Decreasing MgO corresponds with the inception of ferromagnesian mineral fractionation, while the decreasing of Al_2O_3 and CaO are indicative of crystallization of pyroxene and plagioclase.

Trace and rare earth elements

Trace element behavior has been recognized as more sensitive to the process of magma generation and differentiation in basaltic systems (Yoder, 1976). Decoupling of trace elements from major elements contributes to this sensitivity. Trace elements are not as intimately tied with the polymerization of the melt as are the major elements. This results in a greater response of the trace elements to change during magmatic processes.

Variation of trace elements with increasing magmatic differentiation for the Badwater greenstones are indexed with FeO/(FeO + MgO) and are shown in Figure 5. Compatible elements such as Ni and Cr, decrease with increasing differentiation, while the hygromagmatophile elements (Rb, Ba, Zr, Y, etc.) show a trend of enrichment with increasing differentiation. It has been suggested that the elements such as Ti, P, Zr, Hf, Th, Cr, Ni, Sc, Nb, Y, and HREE in basalts are resistant to alteration and metamorphism (Pearce and Cann, 1973; Floyd and Winchester, 1975; Wood *et al.*, 1976; Condie *et al.*, 1977; Ludden and Thompson, 1978; Ludden *et al.*, 1982), while other elements such as Sr, Ca, Ba, K, and Na can be shown to be mobile even during low grade alteration (Humphris and Thompson, 1978). In this study, the LIL (large ion lithophile) elements of the Badwater greenstones show a much wider scattering and poorer correlation as compared to the tight clustering of the immobile elements (e. g., Zr, Y). This suggests that the immobile elements can be used for modelling whereas the LIL, whose scattering is problem due to alteration and metamorphism, may be used with caution.

The REE concentrations were normalized to chondrite values and then plotted logarithmically against atomic number. Plots of chondrite normalized REE data for the Badwater greenstones are shown in Figure 6. The Eu anomalies, positive anomalies in less evolved rocks and showing flat in more evolved rocks, might be suggest that fractionation of plagioclase, which preferentially deprives the melt of Eu under favorable oxygen fugacity conditions.

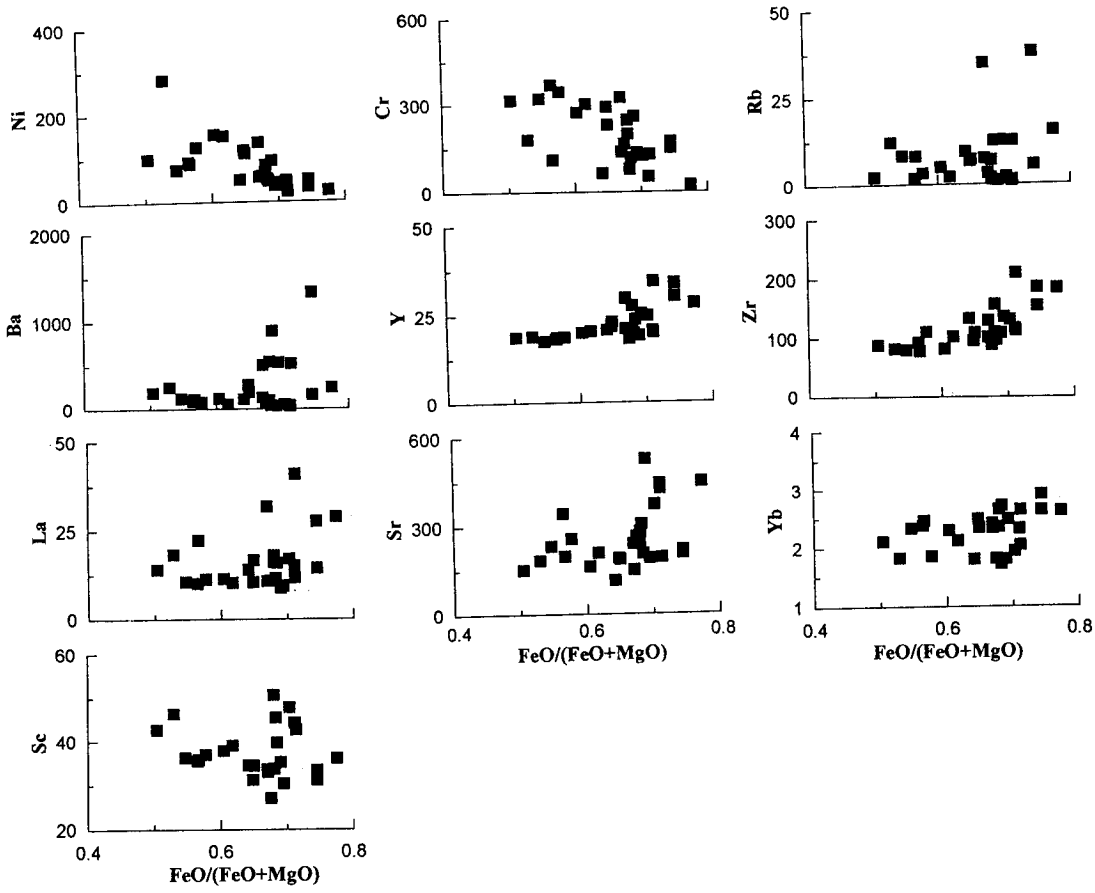

Fig. 5. Variation diagrams of selected trace and rare earth elements vs differentiation index.

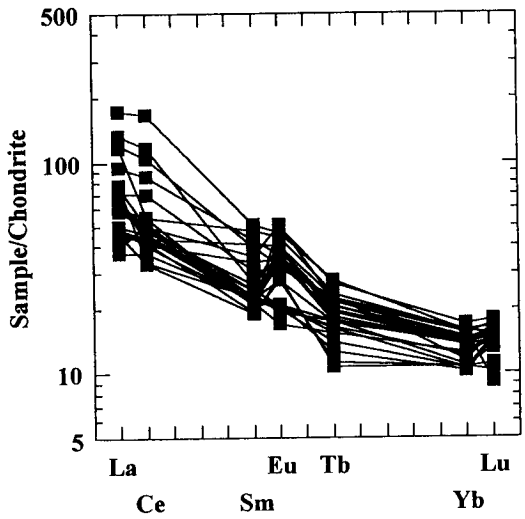

Fig. 6. Chondrite normalized REE patterns of the Badwater greenstones.

DICUSSION

Chemical variation of the evolved rocks

The chemical differentiation of most magmas results from processes operating in the subsurface. Factors controlling their composition include the source composition as well as pressure, temperature, and degree of partial melting of the source. Fractional crystallization and contamination may operate at any level to produce further variation.

Crystal fractionation is one of the major controls on the evolution of Badwater greenstones as supported by the presence of phenocrysts of plagioclase, clinopyroxene, and iron-oxides in the metabasalts. The evaluation of fractional crystallization is best performed on fresh rocks for which original mineral compositions are available. Because of the alteration process, no accurate chemical data for the original minerals are available for these rocks. Thus, I concentrate mainly on the element that appear to be immobile in basaltic

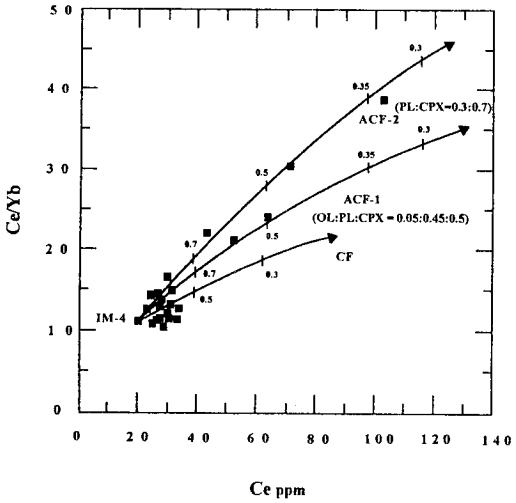

Fig. 7. Ce/Yb vs Ce ppm for the Badwater greenstone. Line CF represents the treand of closed system crystal fractionation model (OL : PL : CPX=0.05 : 0.45 : 0.5), whereas lines ACF1 and ACF2 mark simulations using assimilation crystal fractionation model. Tick on the lines mark fraction of magma remaining.

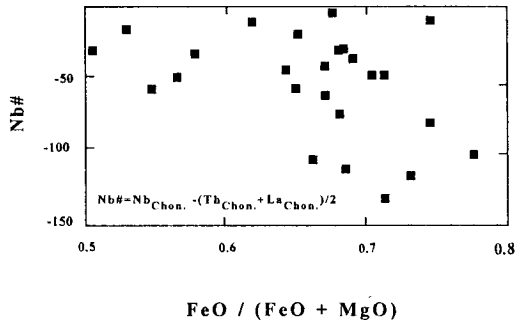

Fig. 8. Plot of Nb# vs. differentiation index for the Badwater greenstones. Nb# is defined as the difference between chondrite normalized Nb abundance and the average of chondrite normalized Th and La.

rocks during weathering and metamorphism.

In order to simulate the solidification history using the Rayleigh fractionation model (Allegre and Minster, 1978), sample IM-4 is chosen here to approximate the starting composition because it has the least differentiated REE composition, low SiO_2 (47.2%), high MgO (9.5%) and Ni (280 ppm) contents. Figure 7 shows Ce/Yb vs Ce ppm plot for the Badwater greenstones. Line CF marks the modelling of the differentiation history using closed system crystal fractionation model, whereas lines ACF1 and ACF2 represent simulations using an assimilation crystal fraction model developed by DePaolo (1981). An assimilation rate of 0.35 is used here because the same number has been successfully applied in modeling the Deccan basalt of India and the Coppermine River basalt of the northwest territories, Canada (Dupuy and Dostal, 1984). Partition coefficients are adopted from Cox *et al.* (1979) and Henderson (1984). Bulk partition coefficients are calculated assuming fractionations of 1) olivine, plagioclase, clinopyroxene in the proportions 0.05: 0.45: 0.5 (D_{Ce}=0.23, D_{Yb}=0.53), and 2) plagioclase and clinopyroxene in the proportions of 0.3 : 0.7 (D_{Ce}=0.28, D_{Yb}=0.72). As shown by the crystal fractionation trend in Figure 7, differentiation by crystal fractionation (assumming fractionation of olivine, plagioclase, and clinopyroxene in the proportions 0.05 : 0.4 : 0.55) alone seems to have difficulty evolving the observed Ce/Yb ratios present in the rocks before major portions of the magma solidified.

Crustal contamination of the basaltic magma during emplacement was considered to explain the excessive enrichment of Ce in the Badwater greenstones. The crustal rocks of the study area have a higher Ce content and Ce/Yb ratios (Ce=50, Yb=1. 7, by average of 3 crustal rocks). Evaluation of the Ce/Yb vs. Ce plot (Figure 7) tends to support the assimilation crystal fractionation (ACF) model. It thus appears that the preferred model to explain the excessive enrichment of Ce in the present study is ACF model and the trend of differentiation can be interpreted to represent ACF rather than simple fractional crystallization.

Geochemical pattern of averaged Badwater greenstones shows distinctive depletion of Nb with respect to its neighboring elements (see Figure 10b). This depletion would require a mineral that selectively removes Nb with respect to other incompatible elements such as Th and La. Although Nb partitions strongly into the Ti-rich minerals such as sphene and rutile (Green and Pearson, 1987), there is no correlation between calculated Nb values $((Nb)_c-[(Th)_c+(La)_c]/2)$ and Ti content. Therefore, the depletion of Nb reflects the contamination of the magma by Nb depleted crustal material. The reason for the depletion of Nb in continental crust has not been known exactly. Recently Hofmann (1988) explained the Nb depletion by a switching of their compatibility during the formation of continental and oceanic crust. Nb was moderately incompatible during the formation of the continental crust (similar to Ce) and becomes highly incompatible (similar to U and K) during the formation of MORB (Hofmann,

1988). Nb # values (Figure 8) for the Badwater greenstones decrease with increasing differentiation index. This implies continuing assimilation throughout the differentiation history.

Geochemical interpretations of tectonic setting

The interpretation of paleoenvironments of basaltic magma generation in the southern Lake Superior region was based on the use of the previously devised discrimination diagrams. Immobile elements are suitable for use in a tectonic discrimination diagrams. What these diagrams do not consider is the temporal decrease in global heat flow. This would have influenced the depth and degree of partial melting of the mantle and the likelihood of contamination by sialic crust. For above reasons, in the diagrams which follow, the field boundaries defined by modern volcanic rocks serve merely as a reference framework to which the Precambrian data can be compared.

Several discrimination schemes utilizing distinctive trace element distributions in mafic volcanics have been proposed to aid in the reconstruction of ancient tectonic settings. The application of such schemes to volcanic rocks of Precambrian age is based on the assumption that the ancient and modern chemical-tectonic systematics of magma genesis are basically the same.

Figure 9a is a plot of Ti vs Zr used by Pharaoh and Pearce (1984). This diagram discriminates between basic and evolved lavas because the dominant crystallizing phases in basic magma (i.e., olivine, pyroxene, plagioclase) have an insignificant effect in the Ti/Zr ratio of the melt. However, when a Ti bearing phase begins to crystallize and the melt evolves from basic to acid, the removal of Ti results in a decrease in the Ti/Zr ratio (Watters and Pearce, 1987). In this diagram, it is apparent that the all rocks fall in the basic lava side and that the rocks plot in the MORB and within plate basalt (WPB) field. ACF processes do not significantly alter the tectonic indicators in the Ti-Zr plot because Zr concentrations are similar in the crustal material and the magmatic differentiates of the intermediate stage (Ueng *et al.*, 1988), and because the tendency to lower the Ti concentration of the magma by assimilating supracrustal rock is overshadowed by an enrichment trend caused by differentiation. Samples were plotted in Ti-Zr-Y (Pearce and Cann, 1973) to distinguish within plate basalt (WPB), ocean-floor basalt (OFB), low-K tholeiites (LKT), and calc-alkaline basalt (CAB) (Figure 9b). The WPB affinity

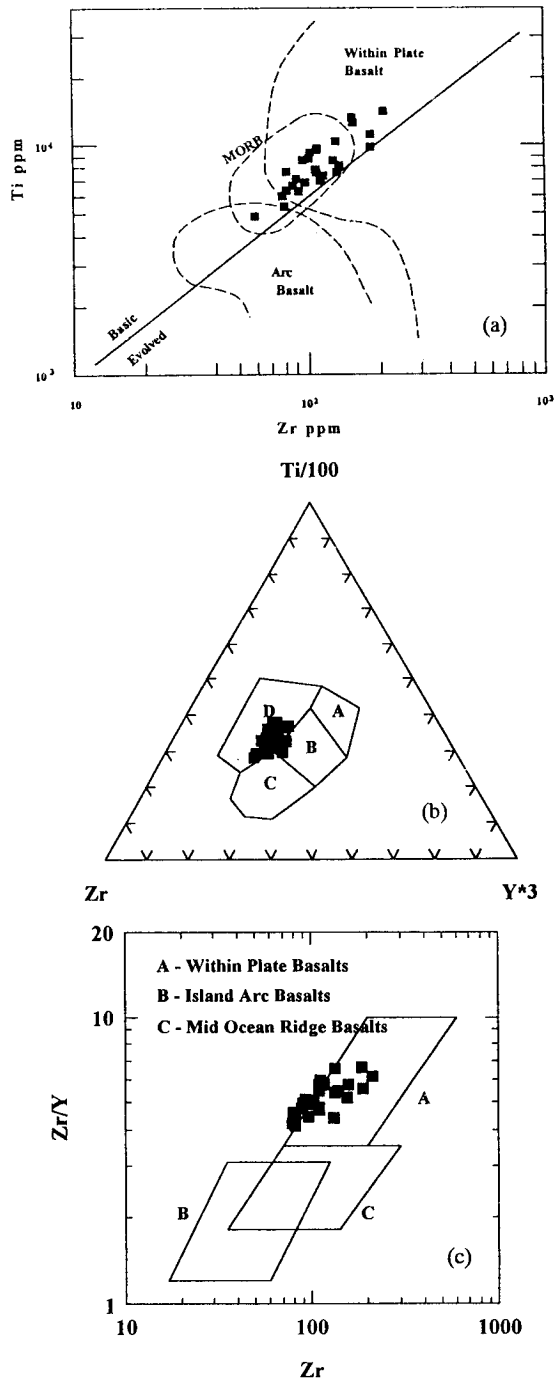

Fig. 9. Tectonic discrimination diagrams for the Badwater greenstones. (a) Ti vs Zr plot. MORE, WPB, and Arc lava fields taken from Pharaoh and Pearce (1984), (b) Ti-Zr-Y polt. A : low-K tholeiitic basalts, B : ocean floor basalts, C : calc-alkaline basalts, D : within plate basalts, (c) logarithm plot of Zr/Y vs Zr.

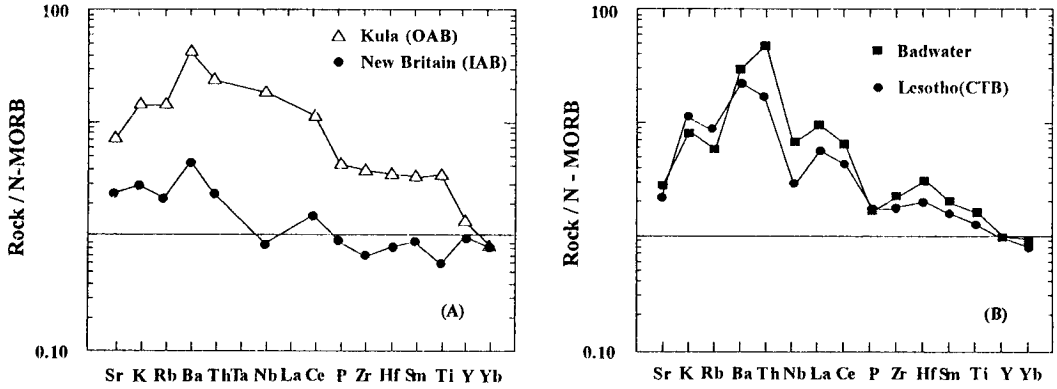

Fig. 10. Geochemical patterns (normalized to N-MORB) of basalts from known tectonic environments. For comparison, averaged Badwater greenstones are presented. Data sourecs for Figure 11a cited in March (1983), and Chen and Frey (1983), 11b cited in Peccerillo and Taylor (1976).

of the rocks is a dominant feature of the plot. However, a fairly large number of rocks plot in the OFB fields. This kind of plot pattern has been interpreted by Morrison (1978) and Holm (1982) as representative of incipient spreading within continental crust. It thus appears that the basaltic rocks plot within and between WPB and OFB on this diagram and suggests that they have characteristic of continental basalts of transitional setting; either continental rifting or back arc basin. Figure 9c (Pearce and Norry, 1979) providing not only a complete separation of WPB and MORB, but effectively distinguishes between these types and volcanic arc basalts. In this diagram, all the rocks are plot within the WPB field.

Based on Figure 9, most of the samples from the Badwater greenstones plotted in either the WPB field or the MORB field. Of particular interest is that the less evolved rocks plot near the MORB field and evolved rocks show a trend into the WPB field as seen in the Zr/Y vs Zr plot. Although these diagrams do not provide a separation of normal MORB (N-type) and plume type MORB (P-type), chemical compositions of the least evolved samples are similar to that of transitional type MORB (T-type) which has relatively low Zr/Nb (7.7~11.8), Y/Nb (1.3~3.0), and slight LREE enrichment ($(La/Yb)_c$=1.7~4.3) ratios (data from LeRoex *et al.*, 1983).

Geochemical pattern of the average composition of the Badwater greenstones was constructed by normalizing to an average N-MORB composition. Patterns for typical basalts from known tectonic settings are presented for comparison. MORB normalized geochemical patterns (Figure 10) provide a useful means of comparing basalts based on the analyzed elements.

Intraplate alkali basalts (Kula in Figure 10a) exhibit an enrichment of all elements relative to N-type MORB, similar to the pattern due to either incompatibilities of the various elements in small degree mantle melts or generated from the enriched mantle source. Compared to N-type MORB, island arc basalts (Figure 10a) are relatively enriched in Sr through Ba and the low content of the immobile elements. Selected modern suites of continental tholeiitic basalts (Figure 10b) erupted in areas of strong lithospheric attenuation also give pattern which exhibit enrichment in the most incompatible elements and depletion in Nb and P with respect to their neighboring elements. It is difficult to chemically distinguish the continental tholeiitic basalt (CTB) and ocean alkali basalt (OAB) with respect to degree of enrichment of overall elements. Both have enriched LIL and HFS elements, however, they show a distinctive difference in the concentration of Nb. The geochemical pattern of the Badwater greenstones (Figure 10b) show very similar distribution pattern and resemble the continental tholeiitic basalts in regard to the degree of enrichment of LIL/HFS elements and Nb and P depletion. The interpretation of these data strongly favor a model of intrusion into a crustal environment undergoing lithospheric attenuation.

CONCLUSIONS

Despite the age and metamorphism of the studied rocks, geochemical analysis, especially for immobile elements, has provided useful information to constrain the petrogenesis of the Badwater greenstones and the paleotectonic environment of the

studied area. Geochemical analyses, tectonic comparisons using diagrammatic methods, and limited chemical modelling of rocks allow the following conclusions :

1. Geochemical data indicate that the Badwater greenstones are tholeiitic; no alkalic basalts were found. The absence of the alkaline basalts within the region might be suggest that early Proterozoic magmas were generated at relatively shallow depths, under the influence of a high geothermal gradient.

2. Geochemical characteristics of the Badwater greenstones show evidence of crustal contamination. Assimilation of crustal rocks have greatly affected elemental abundances, especially in Nb and incompatible elements, which are enriched in crustal rocks. Most of the least evolved rock samples plot in the MORB field in tectonic discrimination diagrams, and these rocks are chemically similar to present day T-type MORB compositions. Thus, with consideration of assimilation effects, it is suggested that the rocks of the study area were derived from a chemically MORB-like, relatively undepleted, lithospheric upper mantle source. The relatively undepleted parent modified by ACF process for the studied rocks and these processes shifted the rock composition to that of continental tholeiites as the rock evolved.

3. Based on all the geochemical characteristics and tectonic discrimination diagrams, the studied rocks emplaced during rifting. The geochemical patterns of these rocks are similar to continental tholeiitic basalts from Lesotho, which erupted in more recent rift environment.

ACKNOWLEDGEMENTS

I would like to thanks the late Dr. J.T. Wilband for all his help, encouragement and advice during the preparation of this study. Helpful and constructive reviews by Prof. S.T. Kwon is greatly appreciated.

REFERENCES

Allegre, C.J., and Minster, J.F. (1978) Quantitative models of trace element behavior in magmatic processes. Earth Planet. Sci. Lett., v. 38, p. 1-25.

Cambray, F.W. (1978) Plate tectonics as a model for the environment of deposition and deformation of the early Proterozoic (Precambrian X) of northern Michigan. Geol. Soc. Am. Abs. w/Prog., v. 10, p. 376.

Cannon, W.F. (1973) The Penokean Orogeny in Northern Michigan. Geol. Asso. Canada, Spec. Pap., v. 12, p. 251-271.

Chen, C.Y., and Frey, F.A. (1983) Origin of Hawaiian tholeiites and alkalic basalts. Nature, v. 302, p. 785-789.

Condie, K.C., Bobrow, D.J., and Card, K.D. (1987) Geochemistry of Precambrian mafic dikes from the southern Superior Province of the Canadian Shield. Geol. Soc. Canada Spec. Pap., v. 34, p. 95-108.

Condie, K.C., Viljoean, M.J., and Kable, E.T.D. (1977) Effects of alteration on element distributions in Archean tholeiites from the Barberton Greenstone Belt, south Africa. Contrib. Mineral. Petrol., v. 64, p. 75-89.

Cox, K.G., Bell, J.D., and Pankhurst, R.J. (1979) The interpretations of igneous rocks. London, Allen and Unwin. 450 pp.

DePaolo, D.J. (1981) Trace element and isotopic effects of combined wallrock assimilation and fractional crystallization. Earth. Planet. Sci. Lett., v. 53, p. 189-202.

Dupuy, C., and Dostal, J. (1984) Trace element geochemistry of some continental tholeiites. Earth Planet. Sci. Lett., v. 67, p. 61-69.

Floyd, P.A., and Winchester, J.A. (1975) Magma type and tectonic setting discrimination using immobile elements. Earth Planet. Sci. Lett., v. 27, p. 211-218.

Fox, T.P. (1983) Geochemistry of the Hemlock metabasalt and Kiernan sills, Iron county, Michigan. M. S. Thesis, Michigan State University, 81p.

Green, T.H., and Pearson, N.J. (1987) An experimental study of Nb and Ta partitioning between Ti-rich minerals and silicate liquids at high pressure and temperature. Geochim. Cosmochim. Acta, v. 51, p. 55-61.

Greenberg, J.K., and Brown, B.A. (1983) Lower Proterozoic volcanic rocks and their settingin the southern Lake Superior district. Geol. Soc. Am. Mem. 160, p. 67-84.

Henderson, P. (1984) Rare earth element geochemistry. Elsevier. Amsterdam. 510 pp.

Hofmann, A.W. (1988) Chemical differentiation of the Earth: the relationship between mantle, continental crust, and oceanic crust. Earth Planet Sci. Lett., v. 90, p. 297-314.

Holm, P.E. (1982) Non-recognition of continental tholeiites using the Ti-Zr-Y diagram. Contrib. Mineral. Petrol., v. 79, p. 308-310.

Honkamo, M. (1987) Geochemistry and tectonic setting of early Proterozoic volcanic rocks in northern Ostrobothnia, Finland, In Geochemistry and Mineralization of Proterozoic volcanic suites. edited by T.C. Pharaoh, R.D. Beckinsale, and D. Rickard, Geol. Soc. Spec. Pub., v. 33, p. 59-68.

Hughes, C.J. (1973) Spilites, Keratophyres, and the Igneous spectrum. Geology Magazine, v. 109, p. 513-527.

Humphris, S.E., and Thompson, G. (1978) Trace element mobility during hydrothermal alteration of oceanic basalts. Geochim. Cosmochim. Acta, v. 42, p. 127-136.

James, H.L., Dutton, C.E., Pettijohn, F.J., and Weir, K. (1968) Geology and ore deposits of the Iron River-Crystal Falls district, Iron county, Michigan. U. S. Geol. Sur. Prof. Pap. 570, 134p.

Larue, D.K. (1983) Early Proterozoic tectonics of the Lake Superior region : Tectonostratigraphic terranes near the purported collision zone. Geol. Soc. America Mem. v. 160, p. 33-47.

Larue, D.K., and Ueng, W.L. (1985) Florence- Niagara terrane, an early Proterozoic accretionary complex, Lake Superior region, U.S.A. Geol. Soc. Am. Bull., v. 96, p. 1179-1187.

LeRoex, A.P., Dick, H.J.B., Erlank, A.J., Reid, A.M., Frey, F.

A., and Hart, S.R. (1983) Geochemistry, Mineralogy and petrogenesis oflavas erupted along the southwest Indian ridge between the Bouvet Triple junction and 11 degrees east. J. Petrol., v. 24, p. 267-318.

Ludden, J.N., Gelinas, L., and Trudel, P. (1982) Archean metavolcanics from the Rouyn-Noranda district, Abitibi greenstone belt, Qubec. 2. Mobility of trace element and petrogenetic constraints. Canadian J. Earth Sci., v. 19, p. 2276-2287.

Ludden, J.N., and Thompson, G. (1978) Behavior of rare earth elements during submarine weathering of sea-floor basalt. Earth Planet. Sci. Lett., v. 43, p. 85-92.

Marsh, J.S. (1987) Basalt geochemistry and tectonic discrimination within continental flood basalt provinces. J. Volcano. Geotherm. Res., v. 32, p. 35-49.

Morrison, M.A. (1978) The use of immobile elements to distinguish the paleotectonic affinities of metabasalts: application to Paleocene basalts of Mull and Skye, N.W. Scotland. Earth Planet. Sci. Lett., v. 39, p. 407-416.

Pearce, J.A., and Cann, J.R. (1973) Tectonic setting of basic volcanic rocksdetermining using trace element analyses. Earth Planet. Sci. Lett., v. 19, p. 290-300.

Pearce, J.A., and Norry, M.J. (1979) Petrogenetic implications of Ti, Sr, Y and Nb variations in volcanic rocks. Contrib. Mineral. Petrol., v. 69, p. 33-47.

Peccerillo, A., and Taylor, S.R. (1976) Geochemistry of Eocene calc-alkaline volcanic rocks from the Kastsmonu area, northern Turkey. Contrib. Mineral. Petrol., v. 58, p. 63-81.

Pharaoh, T.C., and Pearce, J.A. (1984) Geochemical evidence for the geotectonic setting of early Proterozoic metavolcanic sequences in Lapland. Precambrian Res., v. 25, p. 283-308.

Ueng, W.C., Fox, T.P., Larue, D.K., and Wilband, J.T. (1988) Geochemistry and petrogenesis of the early Proterozoic Hemlock volcanic rocks and the Kiernan sills, southern Lake Superior region. Canadian J. Earth Sci., v. 25, p. 528-546.

Van Schmus, W.R. (1976) Early and middle Proterozoic history of the Great Lake area, North America. Phil. Trans. Royal Soc. London, Ser. A, v. 280, p. 605-628.

Watters, B.R., and Pearce, J.A. (1987) Metavolcanic rocks of the La Ronge Domain in the Churchill Province, Saskatatchewan : geochemical evidence for a volcanic arc origin, In Geochemistry and mineralization of Proterozoic volcanic suites. edited by T.C. Pharaoh, R.D. Beckinsale, and D. Rickard, Geol. Soc. Spe. Pub., v. 33, p. 167-182.

Wee, S.M. (1991) Geochemistry of Precambrian mafic dikes in northern Michigan, U.S.A. : Implications for the Paleotectonic environment. J. Korean Inst. Min. Geol., v. 24, p. 447-463.

Wee, S.M. (1993) Geochemical evidence for the tectonic setting of the early Proterozoic metavolcanic sequences in southern Lake Superior region. J. Mineral. Petrol. Econ. Geol., v. 88, p. 320-334.

Wood, D.A., Gibson, I.L., and Thompson, R.N. (1976) Elemental mobility during zeolite facies metamorphism of the Tertiary basalts of eastern Iceland. Contrib. Mineral. Petrol., v. 55, p. 241-254.

Yoder, H.S. (1976) Generation of basaltic magma. National Academy of Sciences, Washington D.C., 265p.

Manuscript received 29 March 1996

위스콘신주 북동부 지역에 분포하는 Badwater녹암에 대한 지화학적 연구

위 수 민

요 약 : 위스컨신주 북동부 지역에 분포하는 Badwater녹암의 암석학적인 특징과 그들이 생성될 당시의 지구조적인 환경을 유추하기 위하여 채취한 암석을 분석하여 지화학적 연구가 행하여 졌다. 암석들의 화학조성은 전형적인 대륙성 쏠레아이트이며, Mg값이나 Ni, Cr과 같은 호정적인 원소의 함량에 미루어 분출되기전에 많은 분별정출작용을 받았음을 시사한다. 암석들의 불호정적원소의 변화를 살펴보면 이들은 지각과의 동화작용에 많은 영향을 받았다고 사료된다. 이 암석들은 다양한 화학조성을 보이고 있으나, 모마그마의 성분과 유사한 가장 덜 분화된 암석은 전이형 해양현무암과 유사한 화학조성을 가지고 있다. 이러한 점으로 미루어 전이형 해양현무암과 화학조성이 유사한 모마그마가 지각과의 동화작용으로 그들의 화학조성이 현재의 대륙성 쏠레아이트와 같이 변하였음을 시사한다. 암석들의 지화학적 특성을 살펴보면 분기지역과 같은 인장력을 받는 지구조적 환경에서 생성된 현무암과 유사한 화학적 특징을 나타낸다.